

Chapter 17. Stable Isotopes as Tracers for Studying Biosphere-Atmosphere Exchange

“Rural air samples were all collected from the layer of air close to the ground ... under circumstances where the metabolic activity of plants might be expected to influence the carbon dioxide composition of the air. This is so because plants exchange carbon dioxide with the atmosphere by means of respiration and assimilation and also because carbon dioxide is evolved from the ground through decay of organic material in the soil and respiration of plant roots ... Thus the relationship between carbon isotope ratio and molar concentration observed for the carbon dioxide of rural air is explained if carbon dioxide is added to or subtracted from the atmosphere by plants or their decay products.”

Charles Keeling (1958)

Scripps Institution of Oceanography

One of the tools that have provided researchers with an integrated perspective on carbon flows through photosynthesis and respiration is stable isotope analysis. As carbon is assimilated from the atmosphere, flows through the photosynthetic and respiratory processes of the leaf, and is then released back to the atmosphere, the ^{13}C and ^{12}C isotopes exhibit different biotic and abiotic fluxes, causing isotopic fractionations. Analysis of those fractionations has provided valuable insight into the various biogeochemical processes that control the concentration of CO_2 in the atmosphere. Connections between the isotopic composition of atmospheric CO_2 and biospheric processes were recognized in the studies conducted several decades ago by Charles Keeling, a geochemist at the California Institute of Technology, who systematically collected and analyzed the isotopic state of the atmosphere above both terrestrial and marine ecosystems. Keeling not only pioneered the use of stable isotope analysis as a biogeochemical tool, but he made several fundamental discoveries about dynamics in the photosynthetic and respiratory activities of plants and soil in response to climate variation.

In this chapter we cover aspects of stable isotope fractionation by biogeochemical processes and discuss the application of stable isotope analysis at scales ranging from cells to landscapes. Much of the carbon isotope fractionation that occurs begins with the diffusion of CO_2 into leaves and its subsequent assimilation through photosynthetic biochemistry. Thus, we

will begin our discussion with photosynthetic enzymes and their tendencies toward discriminating against the different isotopic forms of CO₂. Following its assimilation into the organic fraction of the biosphere, carbon can be released back to the atmosphere through plant and microbial respiratory processes that also have potential for isotopic fractionation. This respiratory fractionation is not necessarily associated with enzyme active sites, and to understand its nature we need to also understand the potential for molecular structure and the systematic, but differential distribution of ¹³C and ¹²C in the organic molecules that serve as respiratory substrates. As the scale at which isotopic ratios are observed increases, the biochemical processes that influence carbon isotopic fractionation must be integrated into a broader perspective that includes biophysics and micrometeorology. Thus, diffusive fractionation at the scale of leaves and the vertical mixing of different carbon isotope sources within the atmospheric mixed layer must be considered in larger scale analyses. Finally, as we expand the analysis of carbon isotope ratios to the scale of entire ecosystems and landscapes, soil processes, must also be reconciled. We will take this sequence of progressively larger spatial scales and their associated fractionation processes as a framework within which to develop the topic of stable isotope analysis. Most of our discussion will focus on carbon isotopes and their relevance to photosynthesis, respiration and regional-to-global carbon cycling.¹ However, we will also devote some discussion to processes that affect the differential ratios of oxygen isotopes within CO₂, but once again with the aim being to better understand carbon cycling processes. As with previous chapters, one of the principal themes we will adhere to as we develop these topics is the requirement for conservation of mass as a foundation for the theoretical underpinnings of mass exchanges between different components of an ecosystem.

17.A. Stable isotope discrimination by Rubisco and at other points in plant carbon metabolism

Many years ago, Nier and Gulbransen (1939) reported the intriguing observation that the abundance of ¹³C and ¹²C varied in natural materials, and Wickman (1952) reported variation of the ¹³C/¹²C ratio in different plant species. We now understand that much of the variation that was observed in these early studies is due to kinetic isotope effects that result from (1) the differential diffusion rates of ¹³CO₂ and ¹²CO₂ during photosynthetic CO₂ assimilation, *and* (2) the tendency for carboxylation enzymes to favor one isotopic form over the other as

photosynthetic substrates. In C_3 plants, the carboxylation isotope effect is due to discrimination by the enzyme Rubisco (see Section 3.D).

The photosynthetic reaction catalyzed by Rubisco exhibits a relatively large kinetic isotope effect favoring the assimilation of $^{12}\text{CO}_2$ relative to $^{13}\text{CO}_2$, $\alpha \approx 1.030$ ($\Delta \approx 30 \text{ ‰}$). The reaction sequence by which Rubisco catalyzes CO_2 assimilation is characterized by two sequential steps: (1) deprotonation of RuBP to form the reactive enediolate and, (2) covalent bond formation between the enediolate and the carbon atom contained in CO_2 . (Recall that the enediolate is an intermediate compound formed from RuBP within the active site of Rubisco, and which is highly reactive with CO_2 that enters the active site; see Section 4.B.3.) The kinetic isotope effect, which favors the assimilation of $^{12}\text{CO}_2$, occurs during the second step in the reaction sequence; that involving the formation of a bond between the enediolate and CO_2 . The activation energy required for bond formation between $^{12}\text{CO}_2$ and the RuBP enediolate is lower than for $^{13}\text{CO}_2$; thus, reaction rates are faster for $^{12}\text{CO}_2$, leading to discrimination against $^{13}\text{CO}_2$. (It is common for lighter isotopic forms of compounds to be favored in the catalyzed formation of covalent bonds; see Section 3.E.) There is some room for variation among the Rubiscos of different organisms in the magnitude of this isotope effect. For example, the effect will be slightly larger if the covalent bond forms late in the process by which the enediolate is strained toward forming the transition state (Tcherkez et al. 2006); the dynamics of enediolate strain are determined to large extent by the amino acid composition and sequence in the active site of the protein. The range of discrimination for Rubisco observed among a diverse selection of photosynthetic organisms ranging from bacteria to vascular plants is as low as $\sim 20 \text{ ‰}$ and as high as 32 ‰ (Tcherkez et al. 2006). For vascular, C_3 plants, carbon isotope discrimination values by Rubisco extracted from leaves and observed *in vitro* have been reported to range from $27.4 - 30.3 \text{ ‰}$ (Christeller et al. 1976, Roeske and O'Leary 1984, Guy et al. 1993, McNevin et al. 2007). Many past treatments have used a value of 29 ‰ as typical of C_3 Rubisco carbon isotope discrimination; though Farquhar et al. (1989) argued that this value should be reduced by approximately 1.9 ‰ when placed into the context of a C_3 leaf because of the compensatory effects of carboxylation by PEP carboxylase, which is active albeit at low levels in most C_3 species. Thus, in most recent treatments, a value of 27 ‰ has been used for the biochemical discrimination in C_3 leaves. This can be considered a 'maximum' biochemical discrimination value, obtainable when diffusion processes do not limit the process.

The actual discrimination expressed by Rubisco in C_3 leaves (the *in vivo* discrimination) is considerably less than the maximum of 27 ‰ because of leaf diffusive limitations. In order for full discrimination to be expressed at the active site of Rubisco, any $^{13}\text{CO}_2$ that is subjected to discrimination must be free to diffuse away from the reaction. The existence of a diffusive resistance that limits the potential for $^{13}\text{CO}_2$ to leave the site of the reaction will reduce the capacity for biochemical discrimination by Rubisco. Furthermore, the diffusion of $^{13}\text{CO}_2$ and $^{12}\text{CO}_2$ into a leaf will cause some fractionation, due to the fact that their masses are different, and thus they will diffuse at different rates. The combined effect of diffusive limitations will cause the actual discrimination observed during photosynthesis by a leaf to be 14-20 ‰, considerably less than the 27 ‰ estimated for Rubisco limitations alone.

Once assimilated by photosynthetic reactions in the leaf, much of the carbon, now stored in sugars, is oxidized through the processes of respiration in order to provide energy to the cell. Hexose phosphate sugars are oxidized initially in the reactions of glycolysis, and finally in the mitochondrial reactions of the TCA cycle. The product of several of these oxidative steps is CO_2 . If we assume that the initial distribution of ^{13}C and ^{12}C in the sugars produced by photosynthesis is random among the various C atoms, *and* that there is no fractionation associated with respiratory processes, then there should be no difference in the $^{13}\text{C}/^{12}\text{C}$ ratio of photosynthetically-assimilated CO_2 and respired CO_2 . Thus, it was of interest when observations began to emerge showing that respired CO_2 was enriched in ^{13}C , relative to leaf sugars (Ghashghaie et al. 2003, Pataki 2005).

Some progress has been made in determining the cause of the ^{13}C enrichment in respired CO_2 . After careful study, it was discovered that the distribution of ^{13}C and ^{12}C in glucose molecules produced by photosynthesis is not random. For example, the carbon at position 4 in the glucose molecule tends to be enriched in ^{13}C , relative to the overall $^{13}\text{C}/^{12}\text{C}$ of assimilated carbon, while the carbon at position 6 tends to be depleted in ^{13}C (Rossman et al. 1991, Tcherkez et al. 2004). The cause of this non-random distribution is likely to be discrimination that favors ^{13}C in the aldolase reaction of the RPP (C_3) pathway (Gleixner and Schmidt 1997). It is the carbon at position 4 that is lost as CO_2 in the initial step of mitochondrial respiration, resulting in the release of ^{13}C -enriched CO_2 to the atmosphere. The two-carbon molecule that is left behind is depleted in ^{13}C , relative to the original glucose molecule. This molecule, known as acetyl-CoA, enters the TCA cycle, and is oxidized further. If all of the acetyl-CoA molecules were

oxidized to CO₂, there would be no overall enrichment in ¹³C in respired CO₂. However, some of the acetyl-CoA molecules are used in metabolic pathways that branch off from the TCA cycle and are involved in the biosynthesis of lipids and other complex compounds, such as lignin, that contribute plant growth. The carbon used in these branched pathways will be depleted in ¹³C, relative to that lost from carbon 4 as respired CO₂. As we gain more knowledge about the ¹³C/¹²C fractionation patterns in the various photosynthetic and respiratory pathways of a leaf, we will be able to better constrain the metabolic models that we produce to describe carbon partitioning in C₃ plants.

17.B. Fractionation of stable isotopes in leaves during photosynthesis

The relation between diffusion and biochemistry, as leaf processes that fractionate ¹³CO₂ and ¹²CO₂ during photosynthetic CO₂ assimilation, cannot be reconciled as a simple mathematical sum. Rather, discrimination is weighted toward reflecting one or the other process depending on the degree to which each limits the overall rate of net CO₂ assimilation. A mathematical model that describes the relative contributions of both components in C₃ leaves, and has been widely used at scales ranging from leaves to the globe, is stated as (Farquhar et al. 1982):

$$^{13}\Delta = a + (b - a) c_{ic}/c_{ac} \quad (17.1)$$

where ¹³Δ is the overall leaf discrimination against ¹³CO₂, *a* is the discrimination component due to diffusive fractionation and *b* is the discrimination component due to the biochemical reactions of CO₂ assimilation. Equation 17.1 provides a weighting of the diffusive and biochemical discriminatory factors scaled to the ratio of the intercellular CO₂ concentration (*c_{ic}*) to the atmospheric CO₂ concentration (*c_{ac}*). Thus, as *c_{ic}*/*c_{ac}* decreases, the diffusional fractionation becomes more important in determining ¹³Δ and as *c_{ic}*/*c_{ac}* increases the biochemical fractionation becomes more important. It should be noted that this form of the model ignores diffusive fractionation between the intercellular air spaces of the leaf and the site of carboxylation within the chloroplast, as well as fractionation due to the processes of respiration (both 'dark' respiration and photorespiration). We have decided to focus on this simpler form of the model, at least initially, in the interest of establishing the fundamental relations that control fractionation as CO₂

diffuses in and out of a leaf. For a more complete description of fractionation effects in leaves, we refer the reader to Lloyd and Farquhar (1994) and Appendix 17.1. Equation 17.1 contains the implicit recognition that discrimination depends on the capacity for $^{13}\text{CO}_2$ molecules, which accumulate in the intercellular air spaces during photosynthesis, to diffuse back out of the leaf before being assimilated through carboxylation (Fig. 17.1). As the capacity for this 'back-diffusion' decreases, the capacity for Rubisco to discriminate one isotopic form from the other will also decrease. Stated another way, if g_{sc} is low relative to the rate of net CO_2 assimilation, then CO_2 uptake will be limited principally by diffusion, and carboxylation by Rubisco will tend to assimilate $^{13}\text{CO}_2$ at higher rates (less discrimination). As g_{sc} increases, c_{ic} will increase and move closer to c_{ac} , diffusive limitations to CO_2 uptake will be relaxed, $^{13}\text{CO}_2$ will diffuse away from the site of discrimination at higher rates, and Rubisco will assimilate $^{13}\text{CO}_2$ at lower rates (more discrimination). Thus, the degree to which the net CO_2 assimilation rate is limited by diffusion versus biochemistry will be reflected in the c_{ic}/c_{ac} ratio of the leaf, which in turn is reflected in the $^{13}\text{C}/^{12}\text{C}$ ratio of biomass.

On the basis of this theory, we would expect correlations to exist among c_{ic}/c_{ac} , leaf carbon isotope discrimination and photosynthetic water-use efficiency (net CO_2 assimilation rate/transpiration rate; A/E_L) (Farquhar et al. 1989). Carbon isotope ratios are typically expressed in delta notation as:

$$\delta^{13}\text{C}_L = \delta^{13}\text{C}_a - a - (b - a) c_{ic}/c_{ac} \quad (17.2)$$

where, in this case, $\delta^{13}\text{C}_L$ represents the $^{13}\text{C}/^{12}\text{C}$ ratio of the leaf biomass and $\delta^{13}\text{C}_a$ represents the $^{13}\text{C}/^{12}\text{C}$ ratio of the atmosphere, both relative to the commonly accepted Pee Dee Belemnite limestone standard. In leaves, a is estimated as 4.4 ‰, which reflects discrimination proportional to the ratio of the diffusivities of $^{13}\text{CO}_2$ and $^{12}\text{CO}_2$ in air, and b is taken as 27 ‰. The value of $\delta^{13}\text{C}_a$ is -8 ‰ for the well-mixed troposphere. The value of $\delta^{13}\text{C}_L$ typically varies between -20 and -30 ‰, for C_3 plant leaves with the less negative values reflecting lower c_{ic}/c_{ac} and higher diffusional limitations to CO_2 assimilation rate.² The c_{ic}/c_{ac} ratio can be related to leaf photosynthetic water-use efficiency (A/E_L) according to:

$$\frac{c_{ic}}{c_{ac}} = 1 - \frac{1.58 A \Delta c_w}{E_L c_{ac}} \quad (17.3)$$

where Δc_w represents the leaf-to-air water vapor mole fraction difference, A is the CO_2 assimilation rate, E_L is the leaf transpiration rate, and 1.58 represents the ratio of diffusivities for water and carbon dioxide (i.e., K_{dw}/K_{dc}). In order to relate leaf $\delta^{13}\text{C}_L$ to photosynthetic water-use efficiency we must recognize that $\delta^{13}\text{C}_L$ reflects the time-integrated assimilation of CO_2 over the life of the leaf (as well as the import of carbon from other leaves and carbon storage pools), and thus it also reflects the time-integrated mean c_{ic}/c_{ac} and the time-integrated $A \Delta c_w/E_L c_{ac}$ during daytime periods when A is coupled to E_L . According to Equations 17.2 and 17.3, leaves with higher photosynthetic water-use efficiencies should exhibit lower c_{ic}/c_{ac} ratios, and correspondingly higher (less negative) $\delta^{13}\text{C}_L$. This prediction from theory has been supported by independent observations of photosynthetic water-use efficiency in plants (Fig. 17.2). Derivations of Equations 17.1 and 17.3 are provided in Appendix 17.1. General reviews of isotopic fractionation can be found in Rundel et al. (1989), Farquhar et al. (1989), O'Leary (1993) and Lloyd and Farquhar (1994).

17.C. Fractionation of the isotopic forms of H_2O during leaf transpiration

Water that moves through the soil-plant-atmosphere system is, for the most part, composed of the common isotopes of oxygen (^{16}O) and hydrogen (^1H). However, a small fraction is composed of different combinations of the heavier, but rarer, isotopes ^{18}O and ^2H .³ As water evaporates from wet surfaces, two isotope effects (see Section 3.D) will cause water molecules with the heavier isotopes to leave the surface more slowly and thus become concentrated over time in the liquid water that remains behind. A thermodynamic isotope effect occurs because at equilibrium, water with the heavier isotopes will partition into the vapor phase above the surface at a lower $^{18}\text{O}/^{16}\text{O}$ ratio than exists in the liquid phase. A kinetic (non-equilibrium) isotope effect occurs because the binary diffusion rate through air of the heavier isotopic forms of water is less than that of the lighter isotopic forms. The combination of these isotopic effects has been incorporated into a theoretical framework known as the *Craig-Gordon model* (Craig and Gordon 1965):

$$R_E = \frac{1}{\alpha_k} \left(\frac{R_l}{\alpha^*} \frac{1}{(1-h)} - R_a \frac{h}{(1-h)} \right) \quad (17.4)$$

where R_E is the isotopic ratio of evaporated water (e.g., $^2\text{H}_2\text{O}/\text{H}_2\text{O}$ or $\text{H}_2^{18}\text{O}/\text{H}_2^{16}\text{O}$), α_k represents the kinetic effect which is approximated as the ratio of diffusion coefficients K_{dl}/K_{dh} (where K_{dl} and K_{dh} are the diffusion coefficients for water containing the light versus heavy isotopes, respectively), α^* is the thermodynamic fractionation where $\alpha^* = R_l/R_v$, with R_l being the isotopic ratio (heavy/light) in liquid water and R_v being the ratio in water vapor (at equilibrium and with equal temperatures of the liquid and vapor systems), R_l is the isotopic ratio in liquid water at the wet surface, R_a is the isotopic ratio in water vapor of the atmosphere immediately above the surface, and h is the relative humidity of the well-mixed atmosphere above the surface. In Equation 17.4, both α_k and α^* are greater than 1.

The Craig-Gordon model has been adapted to account for the enrichment of leaf water with regard to the heavy isotopes during transpiration. This is accomplished by algebraic rearrangement of Equation 17.4 to solve for R_l , where R_l represents the isotopic ratio of liquid water at the site of evaporation. Recognizing that the mole fraction of water vapor in the leaf intercellular air spaces (c_{iw}) is saturated (i.e., $h = 1$), and assuming no difference in temperature between the leaf and the well-mixed air outside the leaf, we can express the relative humidity of the air outside the boundary layer of the leaf as c_{aw}/c_{iw} . From this point, we can derive an expression analogous to Equation 17.4, but with respect to mole fractions and solving for R_l as:

$$R_l = \alpha^* \left[\alpha_k R_E \left(\frac{c_{iw} - c_{aw}}{c_{iw}} \right) + R_a \left(\frac{c_{aw}}{c_{iw}} \right) \right] \quad (17.5)$$

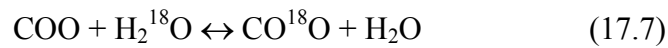
Equation 17.5 has been further modified to account for the serial diffusive resistances provided by stomata and the leaf boundary layer (Flanagan et al. 1991), to provide:

$$R_l = \alpha^* \left[\alpha_k R_E \left(\frac{c_{iw} - c_{sw}}{c_{iw}} \right) + \alpha_{kh} R_E \left(\frac{c_{sw} - c_{aw}}{c_{iw}} \right) + R_a \left(\frac{c_{aw}}{c_{iw}} \right) \right] \quad (17.6)$$

where c_{iw} , c_{sw} and c_{aw} are the mole fractions of water vapor in the leaf intercellular air spaces, at the outer surface of the leaf and in the well-mixed air outside the boundary layer of the leaf, respectively, and α_k and α_{kh} are the kinetic fraction factors in still air and within the leaf boundary layer, respectively.⁴ Kinetic fractionation in the turbulent boundary layer is slightly less than that in still air. A derivation of Equations 17.5 and 17.6 from principles of leaf diffusive fluxes is provided in Appendix 17.2.

17.D. Isotopic exchange of ¹⁸O and ¹⁶O between CO₂ and H₂O in leaves

Interactions between CO₂ and H₂O, facilitated by carbonic anhydrase in the chloroplasts of C₃ leaves (see Section 4.B.2), have also been studied with regard to the fractionation of ¹⁸O and ¹⁶O isotopes in CO₂, and their relation, in turn, to the leaf net CO₂ assimilation rate. Most of the CO₂ molecules that diffuse into a leaf are not assimilated by photosynthesis. Rather, they diffuse back out of the leaf and re-enter the atmosphere. This CO₂ flux is referred to as a “*retroflux*”. Depending on the type of leaf and environmental conditions, the retroflux is between 50-70% of the inward flux (Gillon and Yakir 2001). Before the retrofluxed CO₂ molecules leave the leaf, they may exchange an oxygen atom with H₂O in the leaf’s chloroplasts, catalyzed by the enzyme carbonic anhydrase. Each CO₂ molecule can undergo several hydration reactions during its short residence time in the leaf. During the daylight hours, when evaporative fractionation is significant, the leaf water that hydrates the CO₂ will be enriched with ¹⁸O compared to the water that is conducted into the leaf from the xylem. As a result, retrofluxed CO₂ molecules are ‘tagged’ with an ¹⁸O/¹⁶O ratio that reflects the ¹⁸O enrichment:



As retrofluxed CO₂ molecules leave the leaf they cause an increase in the atmospheric concentration of CO¹⁸O in the vicinity of the canopy. This increase can be viewed as the result of a biophysical discrimination against CO¹⁸O that is dependent on, and proportional to, net CO₂ assimilation rate. In order to develop this relation further, we state the retroflux as:

$$F_r = g_{Lc} c_{cc} \quad (17.8)$$

where F_r is the one-way flux of CO_2 from the chloroplast to the atmosphere ($\text{mol CO}_2 \text{ m}^{-2} \text{ s}^{-1}$), g_{Lc} is the total leaf conductance to CO_2 ($\text{mol air m}^{-2} \text{ s}^{-1}$), and c_{cc} is the CO_2 mole fraction in the chloroplast ($\text{mol CO}_2 \text{ mol}^{-1} \text{ air}$).⁵ The net assimilation rate of CO_2 (A) can be expressed in terms of binary diffusion as:

$$A = -g_{Lc} (c_{ac} - c_{cc}) \quad (17.9)$$

where c_{ac} is the CO_2 mole fraction in the well-mixed atmosphere outside the leaf. Using Equation 17.9 to substitute for g_{Lc} in Equation 17.8, we obtain an expression for the retroflux in terms of the net CO_2 assimilation rate:

$$F_r = -\frac{c_{cc}}{(c_{ac} - c_{cc})} A \quad (17.10)$$

Among different types of plants there are differences in the degree to which retrofluxed CO_2 is isotopically equilibrated with the oxygen atoms in leaf water, due to both differences in leaf carbonic anhydrase activity and in the net CO_2 assimilation rate (Gillon and Yakir 2000, 2001). For example, C_4 grasses generally exhibit less potential for isotopic equilibrium, compared to C_3 grasses (Gillon and Yakir 2001). Given that the coverage by C_4 grasslands in the Northern and Southern Hemisphere subtropics is significant, C_3/C_4 differences in leaf-scale isotopic equilibrium can have large effects on global trends in the isotopic composition of atmospheric CO_2 . The overall global mean fraction of leaf isotopic equilibrium between CO_2 and H_2O is estimated to be 78% (Gillon and Yakir 2001), which is lower than the value of 100% assumed in some previous studies (Farquhar et al. 1993, Cias et al. 1997).

17.E. Assessing the isotopic signature of ecosystem respired CO_2 – the 'Keeling Plot'

In the late 1950's, Charles Keeling recognized that the mathematical relation between CO_2 concentration and the $^{13}\text{C}/^{12}\text{C}$ or $^{18}\text{O}/^{16}\text{O}$ ratios of atmospheric CO_2 is described by a reciprocal linear relation:

$$\delta^{13}\text{C}_a = I(^{13}\text{C}) + M (1/c_{ac}) \quad (17.11)$$

where $\delta^{13}\text{C}_a$ is the isotopic ratio of $^{13}\text{C}/^{12}\text{C}$ in atmospheric CO_2 written in delta notation (see section 3.D), $I(^{13}\text{C})$ is an empirical coefficient that represents the y-intercept of the regression, M is an empirical coefficient that represents the slope of the regression, and c_{ac} is the atmospheric CO_2 mole fraction. At the time of his studies, the CO_2 mole fraction of the well-mixed atmosphere was $314 \mu\text{mol mol}^{-1}$ and Keeling measured a relatively constant, global value for $\delta^{13}\text{C}_a$ of -7‰ at that CO_2 mole fraction. (It is informative for students to ask themselves why the value of $\delta^{13}\text{C}_a$ decreased from -7‰ to -8‰ during the period between 1958 and the present.) In contrast to the constancy that Keeling observed for $\delta^{13}\text{C}_a$ at $314 \mu\text{mol mol}^{-1}$, he noted that the value for $I(^{13}\text{C})$, which represents the $\delta^{13}\text{C}_a$ when the CO_2 mole fraction is extrapolated to really high values (i.e., as $1/c_{ac} \rightarrow 0$), was different for the air above different ecosystems and varied as a function of time of year. Keeling reasoned that the isotopic ratio of CO_2 in air measured at any specific time and for any point in space within the vicinity of an ecosystem ($\delta^{13}\text{C}_a$) must reflect a mixture of ^{13}C and ^{12}C isotope ratios concocted from two CO_2 sources; the well-mixed background (tropospheric) air ($\delta^{13}\text{C}_b$, which at that time was relatively constant at $\sim -7 \text{‰}$) and the CO_2 added from a respiration source within the ecosystem ($\delta^{13}\text{C}_s$, which varies depending on ecosystem type and time of year, but is generally $< -20 \text{‰}$).⁶

We can formalize Keeling's conclusions according to the requirement for conservation of mass in the total CO_2 and isotopic mole fractions, respectively, as:

$$c_{ac} = c_{bc} + c_{sc} \quad (17.12)$$

$$\delta^{13}\text{C}_a c_{ac} = \delta^{13}\text{C}_b c_{bc} + \delta^{13}\text{C}_s c_{sc} \quad (17.13)$$

where c_{ac} , c_{bc} and c_{sc} refer to the CO_2 mole fractions of the atmosphere observed within the vicinity of the ecosystem, the background CO_2 of the well-mixed troposphere, and the CO_2 added from an ecosystem respiration source, respectively (Pataki et al. 2003). Thus, as CO_2 is added to the background atmosphere from a respiratory source, at a different $^{13}\text{C}/^{12}\text{C}$ ratio than that reflected in the background CO_2 , it will change the isotopic composition of the atmospheric CO_2 in the vicinity of an ecosystem in a way that can be described by a linear mixing model:

$$\delta^{13}\text{C}_a = c_{bc} (\delta^{13}\text{C}_b - \delta^{13}\text{C}_s) (1/c_{ac}) + \delta^{13}\text{C}_s \quad (17.14)$$

With this theory in place, one can measure variations in the isotopic composition of CO₂ and CO₂ concentration near the surface of an ecosystem, and through a plot of $\delta^{13}\text{C}_a$ versus $1/c_{ac}$ determine the $\delta^{13}\text{C}$ of ecosystem-respired CO₂; equivalent to the $I(^{13}\text{C})$ of Keeling's original analysis. This type of analysis is best conducted at night, when the surface-atmosphere CO₂ exchange is restricted to respiration. The graphical regression analysis that characterizes the CO₂ concentrations and isotopic compositions of CO₂ according to this theory is called a *Keeling plot* (Fig. 17.3).

Use of the Keeling plot as an analytical tool has allowed scientists to understand the coupling of climate gradients to ecosystem carbon cycling, with dynamics in $\delta^{13}\text{C}_a$ and c_{ac} being the only measured proxies. As discussed above, at the leaf scale, it has been established that increased moisture limitation, either through decreased soil moisture or decreased atmospheric humidity, causes decreased discrimination against ¹³CO₂ (see Section 17.2) This effect has been attributed to increased diffusive limitations in leaves, as stomatal conductance is reduced relative to net photosynthesis rate, and concomitant reductions occur in the ratio of intercellular CO₂ concentration to ambient CO₂ concentration (c_{ic}/c_{ac}). Across spatial and temporal gradients of precipitation, it has been shown that the lower c_{ic}/c_{ac} ratio expected for plants from the drier end of the gradient is correlated with an isotopically 'heavier' (more ¹³C relative to ¹²C) $\delta^{13}\text{C}$ value for the y-intercept of the Keeling plot; thus, reflecting less discrimination against ¹³CO₂ during the photosynthetic production of the sugars that subsequently support ecosystem respiration (see Bowling et al. 2002, Pataki et al. 2003). In this case, we are able to couple process dynamics at the leaf scale with impacts on the local ¹³C/¹²C ratio of atmospheric CO₂.

Two assumptions inherent in the application of the Keeling plot approach are: (1) that only two components are being mixed in linear fashion, the background CO₂ from the well-mixed troposphere and respired CO₂ from the surface, and (2) that the isotopic composition of the two mixed 'end-members' does not change during the analysis (see Pataki et al. 2003). The first assumption forces us to recognize 'ecosystem-respired CO₂' as one pool, despite the fact that it is composed of multiple respiratory components; thus, we cannot distinguish between autotrophic respiration (e.g., rhizospheric respiration) and decomposition respiration. The second

assumption forces us to accept time-dependent error in the analysis and the influence of this non-stationarity on the isotopic fractionation of CO₂ during photosynthesis and respiration. Depending on the magnitude of the environmental forcing on $\delta^{13}\text{C}_s$, the error caused by non-stationarity may be too high to allow us to discern dynamics in the coupling of climate to ecosystem carbon cycling

17.F. The influence of ecosystem CO₂ exchange on the isotopic composition of atmospheric CO₂

As is clear in the examples discussed above, dynamics in the isotopic composition of atmospheric CO₂ have become valuable diagnostics by which to evaluate the influences of climate on ecosystem carbon cycling. Immediately above a terrestrial ecosystem, well removed from the local isotopic influences of oceans, biomass burning or fossil fuel combustion, photosynthetic CO₂ assimilation by plants causes enrichment of atmospheric ¹³CO₂, in the daylight hours, but respiratory use of SOM causes depletion at night.⁷ Theoretically, if the daily photosynthetic and respiratory CO₂ fluxes were tightly coupled, and the ¹³C/¹²C ratios of CO₂ assimilated during the day or respired at night were equal, then the mean diurnal ¹³C/¹²C ratio of air in the vicinity of the ecosystem ($\overline{\delta^{13}\text{C}_a}$) should not change; enrichment with ¹³C during the day should be exactly compensated by depletion with ¹³C at night. This condition can be developed formally from the conservation equation (see Appendix 13.2) assuming a control volume that includes the photosynthetic and respiratory components of the ecosystem as well as the atmosphere immediately above the canopy as:

$$\frac{d\rho_m c_j}{dt} = \frac{\partial \rho_m c_j}{\partial t} + \frac{\partial x}{\partial t} \frac{\partial \rho_m c_j}{\partial x} + \frac{\partial y}{\partial t} \frac{\partial \rho_m c_j}{\partial y} + \frac{\partial z}{\partial t} \frac{\partial \rho_m c_j}{\partial z} \pm \frac{\partial S_{bj}}{\partial z} \pm \frac{\partial S_{cj}}{\partial z} \quad (17.15)$$

where c_j is the mole fraction of atmospheric constituent j , ρ_m is the molar density of air (mol air m⁻³), S_{bj} represents biological sources or sinks of constituent j within the control volume, and S_{cj} represents chemical (reactivity) sources or sinks of constituent j within the control volume (in both cases, the sources and sinks carry units of mol m⁻² s⁻¹, referenced to a unit ground area). Assuming spatial homogeneity such that spatial divergences in the x , y and z coordinates are zero with regard to the transport of CO₂, and with knowledge that CO₂ is chemically stable (such that

$S_{cj} \approx 0$), Equation 17.15 can be simplified to:

$$\frac{d\rho_m c_j}{dt} = \pm \frac{\partial S_{bj}}{\partial z} \quad (17.16)$$

When integrated across the height of the control volume (to reference height z_r) we can write:

$$\int_0^{z_r} \frac{d\rho_m c_{ac}}{dt} dz = \pm \int_0^{z_r} \frac{\partial \bar{S}_{bj}}{\partial z} dz = \int_0^{z_r} \frac{\partial (\bar{A} + \bar{R}_E)}{\partial z} dz = \bar{F}_A + \bar{F}_R \quad (17.17)$$

Term I II III IV

where the time-dependent divergence in the atmospheric CO₂ concentration integrated between height 0 and z_r (Term I), is balanced by the time-averaged biological sink or source activity between height 0 and z_r (Term II), which in this case is equal to the vertically-integrated and time-averaged net photosynthetic (\bar{A}) or ecosystem respiratory (\bar{R}_E) molar fluxes (Term III), which we will designate as \bar{F}_A and \bar{F}_R , respectively (Term IV):

$$\int_0^{z_r} \frac{d\rho_m c_{ac}}{dt} dz = \bar{F}_A + \bar{F}_R \quad (17.18)$$

The fluxes \bar{F}_A and \bar{F}_R are the time-averaged net photosynthetic CO₂ assimilation rate and ecosystem respiration rate, expressed per unit ground area, respectively. When expanded to account for the mole fractions of ¹³C and ¹²C in CO₂, and considering the case for integration with respect to time across a 24-hour cycle, we can write:

$$\int_0^{z_r} \int_0^{24h} \frac{d\rho_m c_{ac} \bar{\delta}^{13}C_a}{dt} dt dz = \bar{\delta}^{13}C_A \bar{F}_A + \bar{\delta}^{13}C_R \bar{F}_R = (\bar{\delta}^{13}C_a - \bar{\Delta}_E) \bar{F}_A + \bar{\delta}^{13}C_R \bar{F}_R = 0 \quad (17.19)$$

where $\bar{\delta}^{13}C_a$ is the mean diurnal ¹³C/¹²C ratio of air in the vicinity of the ecosystem, $\bar{\delta}^{13}C_A$

represents the daily time-averaged $^{13}\text{C}/^{12}\text{C}$ ratio of the photosynthetic products provided by the canopy, $\bar{\delta}^{13}\text{C}_R$ is the daily time-averaged $^{13}\text{C}/^{12}\text{C}$ ratio of the ecosystem respired CO_2 , and $\bar{\Delta}_E$ is the time-averaged photosynthetic discrimination against ^{13}C provided by the ecosystem. Equation 17.19 states the condition of *isotopic equilibrium* between the 24-hour integrated photosynthetic and respiratory components of the ecosystem, which occurs when $\bar{F}_A = \bar{F}_R$ and $\bar{\delta}^{13}\text{C}_A = \bar{\delta}^{13}\text{C}_R$; and thus the mean diurnal change in the $^{13}\text{C}/^{12}\text{C}$ ratio of air in the vicinity of the ecosystem equals zero.

Isotopic equilibrium is not achieved in real ecosystems, even when $\bar{F}_A = \bar{F}_R$. This is due to the fact a unit mass of CO_2 that is photosynthetically removed from the atmosphere at one isotope ratio is replaced by a unit mass of respired CO_2 that exists at a different isotope ratio; in other words, $\bar{\delta}^{13}\text{C}_A \neq \bar{\delta}^{13}\text{C}_R$. The result is *isotopic disequilibrium*. The isotopic ratio of CO_2 produced through soil respiration is affected by the age of SOM pools that serve as substrates and by isotopic fractionation that occurs during respiration. Some of the SOM that contributes to soil respiration is decades old, especially in the slow turnover pool. A considerable fraction of this carbon was assimilated prior to the Industrial Revolution; prior to the large-scale emission of fossilized carbon from coal and oil with their inherently low $^{13}\text{C}/^{12}\text{C}$ ratios (due to ancient photosynthetic discrimination). Because of these emissions, both CO_2 in the atmosphere and the SOM produced from autotrophic biomass have become isotopically ‘lighter’, since the Industrial Revolution. Microbial use of older SOM substrates will result in respired CO_2 that is isotopically heavier, compared to microbial use of younger SOM substrates. The degree of isotopic disequilibrium due to photosynthetic and respiratory activities will be influenced by the relative rates of microbial substrate utilization from SOM pools of different ages. At disequilibrium the left-side term of Equation 17.19 will not equal 0, and the resulting time-dependent change in the $^{13}\text{CO}_2/^{12}\text{CO}_2$ ratio is called the *disequilibrium flux*. The disequilibrium flux is considered for a 24-hour integral in Equation 17.19; but, it can also be defined for the longer time scales associated with processes at larger spatial scales. The presence of an isotopic disequilibrium means that the relative concentrations of carbon isotopes in the CO_2 of the atmosphere could change, despite no change in overall CO_2 mole fraction. The effect of differential oxidation of SOM pools, and its influence on isotopic disequilibrium, must be taken into account for accurate quantification of the effect of soil respiration on the $^{13}\text{CO}_2/^{12}\text{CO}_2$

composition of the atmosphere (Fung et al. 1997). Past efforts have relied on dynamic models of SOM oxidation that provide turnover times for each SOM pool, which are then coupled to predicted changes in the $^{13}\text{C}/^{12}\text{C}$ ratio of atmospheric CO_2 , and thus provide the disequilibrium flux (Ciais et al. 1999, Scholze et al. 2008).

The concept of isotopic equilibrium is illustrated at the global scale in Figure 17.5. The decrease in the $\delta^{13}\text{C}_b$ ratio (and $\delta^{14}\text{C}_b$ ratio) of the background atmosphere due to the combustion of fossil fuels over the past two centuries is estimated according to Francey et al. (1999), and is commonly referred to as the *Suess effect* (Keeling 1979, Tans et al. 1979). Over this same time, the $\delta^{13}\text{C}$ ratio of photosynthate would have tracked that of the atmosphere, but with an offset due to photosynthetic discrimination of $\sim 18 \text{‰}$ (globally averaged and including weighted discrimination by both C_3 and C_4 dominated ecosystems); if isotopic equilibrium were to exist, then the change in the $\delta^{13}\text{C}$ of photosynthate as a function of time (shown in Figure 17.5), should equal the change in $\delta^{13}\text{C}_s$, the globally-averaged $^{13}\text{C}/^{12}\text{C}$ ratio of the respiratory CO_2 source. In the presence of isotopic disequilibrium, the change in $\delta^{13}\text{C}_s$ is lagged by several years, dependent on the globally-averaged residence time of SOM. In this analysis we have presented two alternative residence times for global SOM (τ); 18 years (after Randerson et al. 1999) and 27 years (after Yakir 2004). The effect of an increase in estimated residence time is clearly seen as causing an increase in isotopic disequilibrium; the isotopic disequilibrium with $\tau = 18$ years (D_{18}) is estimated as 0.4 ‰, whereas with $\tau = 27$ years (D_{27}) it is estimated as 0.6 ‰. This small difference underscores the importance of accuracy in estimating the global disequilibrium flux; an estimate that is highly dependent on our understanding of global patterns and rates in SOM decomposition.

Isotopic disequilibrium is also affected by enrichment in ^{13}C that occurs in SOM during mineralization; this is often observed as a 1-3 ‰ increase in $\delta^{13}\text{C}$ of SOM as a function of depth in forest soils (Nadelhoffer and Fry 1988) (Fig. 17.6). Deeper SOM is also older, so some of the increase in $\delta^{13}\text{C}$ can be attributed to CO_2 assimilation in a pre-industrial atmosphere. However, this can only account for, at most, $\sim 1.4 \text{‰}$ of observed increases. The residual difference may be due to: (1) the fact that plant biomass tends to be isotopically lighter than microbial biomass, SOM is composed of progressively higher fractions of microbial biomass as it is processed through time, and the mean age of SOM in deeper soil horizons is older than that for shallower

horizons, and/or (2) microbes discriminate against ^{13}C during SOM oxidation (Ehleringer et al. 2000, Torn et al. 2002). These natural fractionations that occur during SOM mineralization, and differential use of SOM pools to support soil respiration, cannot account for the Suess effect; such differential use would have occurred prior to, as well as after, the Industrial Revolution, so there is no basis to explain shifts in the $^{13}\text{C}/^{12}\text{C}$ ratio of atmospheric CO_2 during the past several decades. However, the presence of this SOM-dependent fractionation does make it more difficult to assess the Suess effect as it is carried forward in time. (By this point in the discussion students should have already recognized the answer to the question posed above as to why the $\delta^{13}\text{C}_a$ observed by Keeling in 1958 as -7‰ has decreased to its current value of -8‰ .)

An additional isotopic tool that can be used to study the turnover rates of SOM involves the quantification of ^{14}C (Trumbore 2000). In SOM with residence times of centuries to millennia, age can be determined by the rate of radioactive decay of ^{14}C , which exhibits an isotopic half-life of $\sim 5,700$ years. However, ^{14}C abundance can also be used in a slightly different way, permitting the estimation of turnover times for much younger SOM pools. During the period 1959-1963, ^{14}C was introduced into the atmosphere as a result of aboveground atomic bomb testing. This pulse of ^{14}C was assimilated into the biosphere through photosynthesis and can be used as a natural tracer to estimate carbon compound turnover times as it moves through pools of leaves, litter and SOM (Goh et al. 1976). In the soil of a deciduous oak-maple forest in the northeastern U.S., for example, the ^{14}C content of various SOM pools was used to estimate turnover times of 2-5 years for leaf litter, 5-10 years for root litter, 40-100 years for low-density humified SOM, and > 100 years for mineral-associated SOM (Gaudinski et al. 2000). In the same study, ^{14}C was used to show that CO_2 derived from SOM that was 1 year or greater in age represented $\sim 40\%$ of the annual soil respiration flux.

Appendix 17.1 Derivation of the Farquhar et al. (1982) model and future augmentations for leaf carbon isotope discrimination

The following derivation of a model to relate the $^{13}\text{CO}_2/^{12}\text{CO}_2$ ratio of photosynthetically-assimilated carbon to the time-averaged c_{ic}/c_{ac} ratio, and thus photosynthetic water-use efficiency, is based on that presented in Farquhar et al. (1982). The rate of $^{12}\text{CO}_2$ diffusion into a leaf can be represented as:

$$A = g_{sc} (c_{ac} - c_{ic}) \quad (17.20)$$

The rate of $^{12}\text{CO}_2$ carboxylation by Rubisco can be represented as:

$$A = k c_{ic} \quad (17.21)$$

where k is a composite biochemical 'transfer coefficient' that we will use for the moment to hold the processes true to form, but which will be eventually cancelled out. Substituting A/k for c_{ic} in Equation 17.21, and using algebra, we obtain:

$$A = \frac{k g_{sc}}{k + g_{sc}} c_{ac} \quad (17.22)$$

We can write the same equations for the diffusion of $^{13}\text{CO}_2$ into a leaf and subsequent carboxylation, but using 'primes' to distinguish from $^{12}\text{CO}_2$:

$$A' = g_{sc}' (c_{ac}' - c_{ic}'); \quad A' = k' c_{ic}'; \quad A' = \frac{k' g_{sc}'}{k' + g_{sc}'} c_{ac}' \quad (17.23)$$

Taking into account the discrimination against $^{13}\text{CO}_2$, relative to $^{12}\text{CO}_2$ by diffusion and Rubisco carboxylation, respectively, we can relate g_{sc}' and k' to g_{sc} and k according to:

$$g_{sc}' = g_{sc} (1 - a/1000) \quad (17.24)$$

$$k' = k(1 - b/1000) \quad (17.25)$$

where a is the steady-state fractionation of $^{13}\text{CO}_2$, relative to $^{12}\text{CO}_2$, due to diffusion through air, and b is the steady-state fractionation of $^{13}\text{CO}_2$, relative to $^{12}\text{CO}_2$, due to discrimination by the active site of Rubisco; both in units of parts per thousand. Using all of these relationships we can write:

$$\frac{A'/A}{c_{ac}'/c_{ac}} = \frac{k'(1 - a/1000) + g_{sc}'(1 - b/1000)}{k' + g_{sc}'} \quad (17.26)$$

The overall discrimination against $^{13}\text{CO}_2$ relative to $^{12}\text{CO}_2$ ($^{13}\Delta$) can be written as:

$$^{13}\Delta = \left(1 - \frac{A'/A}{c_{ac}'/c_{ac}}\right) \times 1000 \quad (17.27)$$

and using Equation (17.26) for substitution we can write:

$$^{13}\Delta = \frac{k'a + g_{sc}'b}{k' + g_{sc}'} \quad (17.28)$$

Recognizing that $g_{sc}' = A'/(c_{ac}' - c_{ic}')$ and $A' = k' c_{ic}'$, we can write $g_{sc}' = k' c_{ic}'/(c_{ac}' - c_{ic}')$, and after substituting into Equation (17.28), and recognizing that $c_{ic}'/c_{ac}' \approx c_{ic}/c_{ac}$, we obtain:

$$^{13}\Delta = a + (b - a) c_{ic}/c_{ac} \quad (17.29)$$

The atmosphere has a $\delta^{13}\text{C}$ value that is approximately 8 ‰ more negative than the PDB standard that is typically used as the reference point for $^{13}\text{C}/^{12}\text{C}$ ratios, and so the isotopic ratio of the leaf, relative to the PDB standard is expressed as:

$$\delta^{13}\text{C}_L = \delta^{13}\text{C}_a - a - (b - a) c_{ic}/c_{ac} \quad (17.30)$$

It should be recognized that the isotopic composition of the leaf is the result of assimilation processes over the entire life of the leaf, as well as any influences due to the import of carbon from other parts of the plant. Thus, the relevant c_{ic}/c_{ac} in Equation (17.30) is the time-integrated value determined for the entire life of the leaf, and for other assimilatory organs that transport carbon into the leaf.

The relationship between c_{ic}/c_{ac} and photosynthetic water-use efficiency can be appreciated if we state:

$$\begin{aligned} A &= g_{sc} (c_{ac} - c_{ic}) \\ E_L &= 1.58 g_{sc} \Delta c_w \end{aligned} \quad (17.31)$$

Using the definition of photosynthetic water-use efficiency as A/E_L , we can state:

$$\frac{A}{E_L} = \frac{g_{sc} c_{ac} - g_{sc} c_{ic}}{1.58 g_{sc} \Delta c_w} \quad (17.32)$$

Using algebra to rearrange Equation 17.32, we can write:

$$1 - \frac{1.58 A \Delta c_w}{c_{ac} E_L} = \frac{c_{ic}}{c_{ac}} \quad (17.33)$$

We have simplified much of the theory to this point by focusing on the relation between $^{13}\text{CO}_2$ and $^{12}\text{CO}_2$ exchange between the ambient atmosphere and the air of the leaf intercellular air spaces. This form of the theory allows us to develop the concepts between $^{13}\text{C}/^{12}\text{C}$ fractionation and leaf water-use efficiency in a straightforward manner. A more detailed treatment of leaf isotopic fractionation would develop the transport pathway from the ambient atmosphere to the chloroplastic site of carboxylation, as well as accounting for other metabolic processes in the leaf that discriminate against ^{13}C . Following Lloyd and Farquhar (1994) we can write an augmented form of Equation 17.29 as:

$$^{13}\Delta = a_b \frac{c_{ac} - c_{sc}}{c_{ac}} + a \frac{c_{sc} - c_{ic}}{c_{ac}} + a \frac{c_{ic} - c_{wc}}{c_{ac}} + (e_s + a_s) \frac{c_{wc} - c_{cc}}{c_{ac}} + b \frac{c_{cc}}{c_{ac}} - \frac{e R_d / (k + f \Gamma_*)}{c_{ac}} \quad (17.34)$$

where a_b is the fractionation of $^{13}\text{CO}_2$ during diffusion across the leaf boundary layer (2.9 ‰), c_{ac} , c_{sc} , c_{ic} , c_{wc} and c_{cc} are the average CO_2 mole fractions in the well-mixed atmosphere, at the surface of the leaf, in the leaf intercellular air spaces, at the wall of mesophyll cells, and in the chloroplast, respectively, e_s is the equilibrium fraction associated with CO_2 solubility into the aqueous phase of the cells, a_s is the fractionation during diffusion in the soluble phase, e and f are fractionations associated with ‘dark’ respiration and photorespiration, respectively, R_d is the dark respiration rate from the tricarboxylic acid cycle, Γ_* is the photocompensation point (i.e., the CO_2 compensation point in the presence of CO_2 efflux from only photorespiration), and k is a biochemical ‘transfer coefficient’, in this case, defined as the carboxylation efficiency (according to $A = k c_{cc}$, or more formally as v_{c1}/c_{cc} where v_{c1} is the RuBP carboxylation rate when not limited by RuBP substrate availability, see Section 5.A.1). In some cases, and in fact to account more accurately for biochemical processes, b is calculated as an ‘effective’ biochemical fractionation combining several processes:

$$b = b_3 - \beta(b_3 - b_4) \quad (17.35)$$

where by convention, b_3 refers to the carboxylation process that leads to a stable 3-C product (i.e., phosphoglyceric acid) and is the fractionation caused by the active site of Rubisco using soluble CO_2 as substrate (taken as 29 ‰), b_4 refers to the carboxylation process that leads to a stable 4-C product (i.e., oxaloacetic acid) and is the fractionation due to carboxylation catalyzed by the cytosolic enzyme phosphoenolpyruvate (PEP) carboxylase including the equilibrium fractionation associated with the reaction of CO_2 with H_2O (because PEP carboxylase uses HCO_3^- as substrate rather than CO_2) (taken as -5.7 ‰), and β is the ratio of PEP to RuBP carboxylation rates in C_3 leaves (typically less than 0.10). Using this approach a value for b can be approximated as 27 ‰ at 25°C.

The fractionations associated with mitochondrial respiration (e) and photorespiration (f) in the right-hand term of Equation 17.34 are not well constrained compared to the other principal fractionations associated with leaf net CO_2 assimilation. It is known that mitochondrial

respiration (R_d) during the night results in ^{13}C -enriched CO_2 (see Section 17.A). However, during the day, mitochondrial respiration rates are down-regulated, and in fact recent observations have suggested that day-respired CO_2 (which includes photorespiration) is depleted in ^{13}C , not enriched (Tcherkez et al. 2010). Thus, the value of e during the day and night is uncertain. In the process of photorespiration, glycine decarboxylase, the enzyme-catalyzed step that releases CO_2 , discriminates against ^{13}C . Both theoretical and empirical studies have estimated that the value of f is related to both the $^{13}\text{C}/^{12}\text{C}$ ratio of recently-assimilated photoassimilates (which enters photorespiration as oxygenated RuBP) and discrimination by glycine decarboxylase; estimates of f range between 7.5 and 13.7 ‰, with 11.5 ‰ being a 'reasonable' first approximation (Lanigan et al. 2008). A discussion of the photocompensation point (Γ^*) can be found in Section 5.C.1.

Appendix 17.2. Derivation of the leaf form of the Craig-Gordon model for H₂O isotopic fractionation

Following Flanagan et al. (1991), the total rate of transpiration from a leaf (E_L) and the rates of transpiration of the heavy (E_L') and light (E_L'') isotopic forms of water can be expressed, respectively, as:

$$E_L = g_L (c_{iw} - c_{aw}) \quad (17.36)$$

$$E_L' = g_L' (R_{iv} c_{iw} - R_{av} c_{aw}) \quad (17.37)$$

$$E_L'' = g_L'' \left[(1/R_{iv}) c_{iw} - (1/R_{av}) c_{aw} \right] \quad (17.38)$$

where g_L , g_L' and g_L'' are leaf conductances to total water vapor (heavy plus light), heavy and light isotopic forms of water vapor, respectively, R_{iv} is the isotopic ratio (heavy/light) of water vapor in the intercellular air spaces of the leaf, and R_{av} is the isotopic ratio (heavy/light) of water vapor in the well-mixed air outside the leaf. Given that $E_L'' \approx E_L$, we can state that $E_L'/E_L'' \approx E_L'/E_L$. Defining α^* as the thermodynamic fractionation factor (where $\alpha^* = R_l/R_v$, and R_l and R_v are the isotopic ratios in the liquid and vapor phases, respectively), and α_k as the kinetic fractionation factor (where $\alpha_k = g_l/g_l'$), we can write:

$$R_l \approx \frac{E_L'}{E_L} = \frac{1}{\alpha_k} \frac{(R_{iv} c_{iw} - R_{av} c_{aw})}{(c_{iw} - c_{aw})} = \frac{1}{\alpha_k} \frac{\left(\frac{R_l}{\alpha^*} c_{iw} - R_{av} c_{aw} \right)}{(c_{iw} - c_{aw})} \quad (17.39)$$

During steady-state transpiration, and recognizing the constraint of mass balance, the isotopic composition of xylem water in the leaf (R_X) must equal that of the water transpired from the leaf; thus, $R_l = R_X$. Substituting R_X for R_l on the left side of Equation 17.5, and rearranging to solve for R_l on the right side of Equation 17.39, we can write:

$$R_l = \alpha^* \left[\alpha_k R_X \left(\frac{c_{iw} - c_{aw}}{c_{iw}} \right) + R_A \left(\frac{c_{aw}}{c_{iw}} \right) \right] \quad (17.40)$$

In still air, the values of α_k for the differential diffusion of water containing the heavy or light

isotopes of hydrogen and oxygen, respectively, are $H_2O/{}^2H_2O = 1.025$ and $H_2{}^{16}O/H_2{}^{18}O = 1.0285$ (Merlivat 1978). Within the turbulent boundary layer of the leaf, the values for α_k (represented as α_{kh}) for both H_2O versus 2H_2O and $H_2{}^{16}O$ versus $H_2{}^{18}O$ are reduced due to advective transfer of the isotopes, which is not subject to mass fractionation, and from the principles of fluid mechanics can be estimated as $H_2O/{}^2H_2O = 1.017$ and $H_2{}^{16}O/H_2{}^{18}O = 1.0189$ (see Flanagan et al. 1991). Thus, Equation 17.40 can be further modified to account for the leaf boundary layer, as:

$$R_l = \alpha^* \left[\alpha_k R_x \left(\frac{c_{iw} - c_{sw}}{c_{iw}} \right) + \alpha_{kh} R_x \left(\frac{c_{sw} - c_{aw}}{c_{iw}} \right) + R_A \left(\frac{c_{aw}}{c_{iw}} \right) \right] \quad (17.41).$$

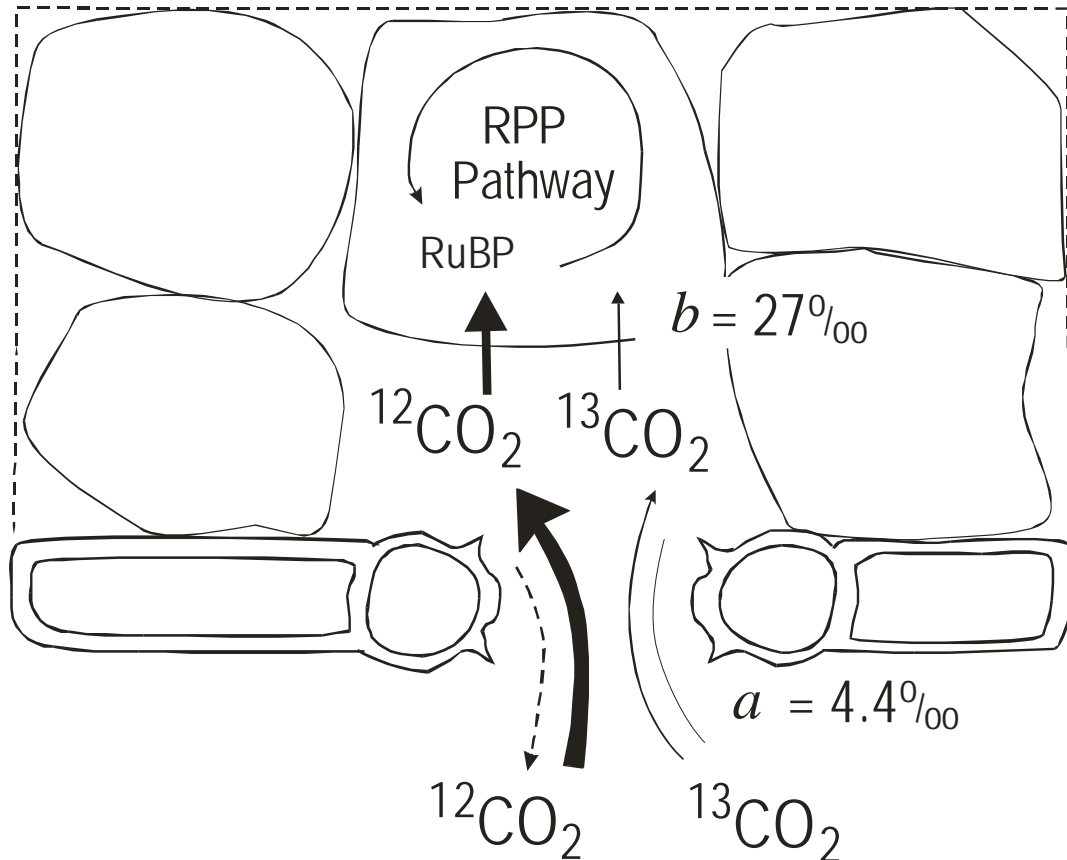


Figure 17.1. Representation of a leaf cross-section showing the diffusive and biochemical paths for the photosynthetic assimilation of $^{13}\text{CO}_2$ and $^{12}\text{CO}_2$. The diffusive and biochemical components of the leaf $^{13}\text{CO}_2$ discrimination are represented as a and b , respectively. Note that the c_{ic} and capacity for Rubisco to discriminate against $^{13}\text{CO}_2$ will depend on g_{sc} and the capacity for $^{13}\text{CO}_2$ that is subjected to discrimination to diffuse back out of the leaf prior to being assimilated by Rubisco. The ultimate carbon isotope ratio of the assimilated carbon will depend on the relative degrees to which diffusion (reflected in a) versus biochemistry (reflected in b) limit the rate of CO_2 assimilation.

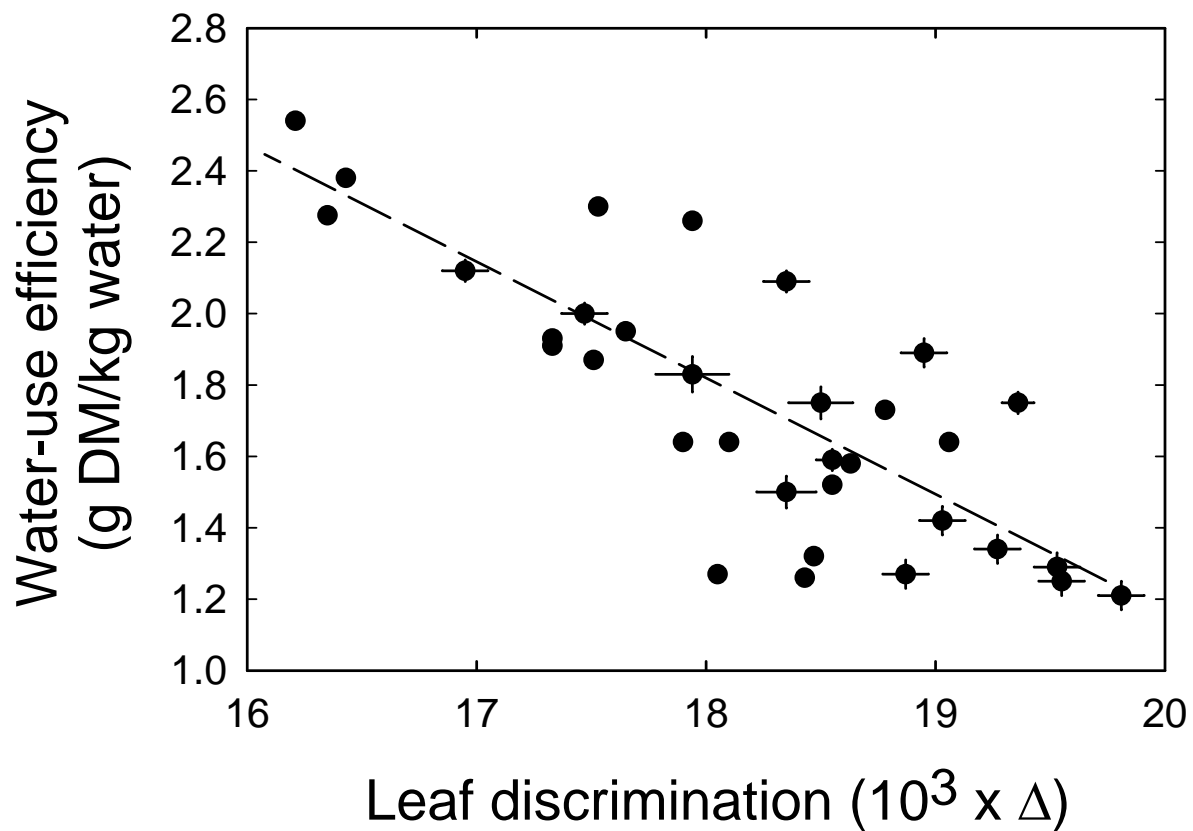


Figure 17.2. Observed relationship between the water-use efficiency of peanut plants, measured as the amount of dry mass (DM) gained per unit of water transpired, and the isotopic discrimination against ¹³CO₂ obtained from the δ¹³C_L. Data for different peanut genotypes have been pooled. Redrawn from Hubick et al. (1986).

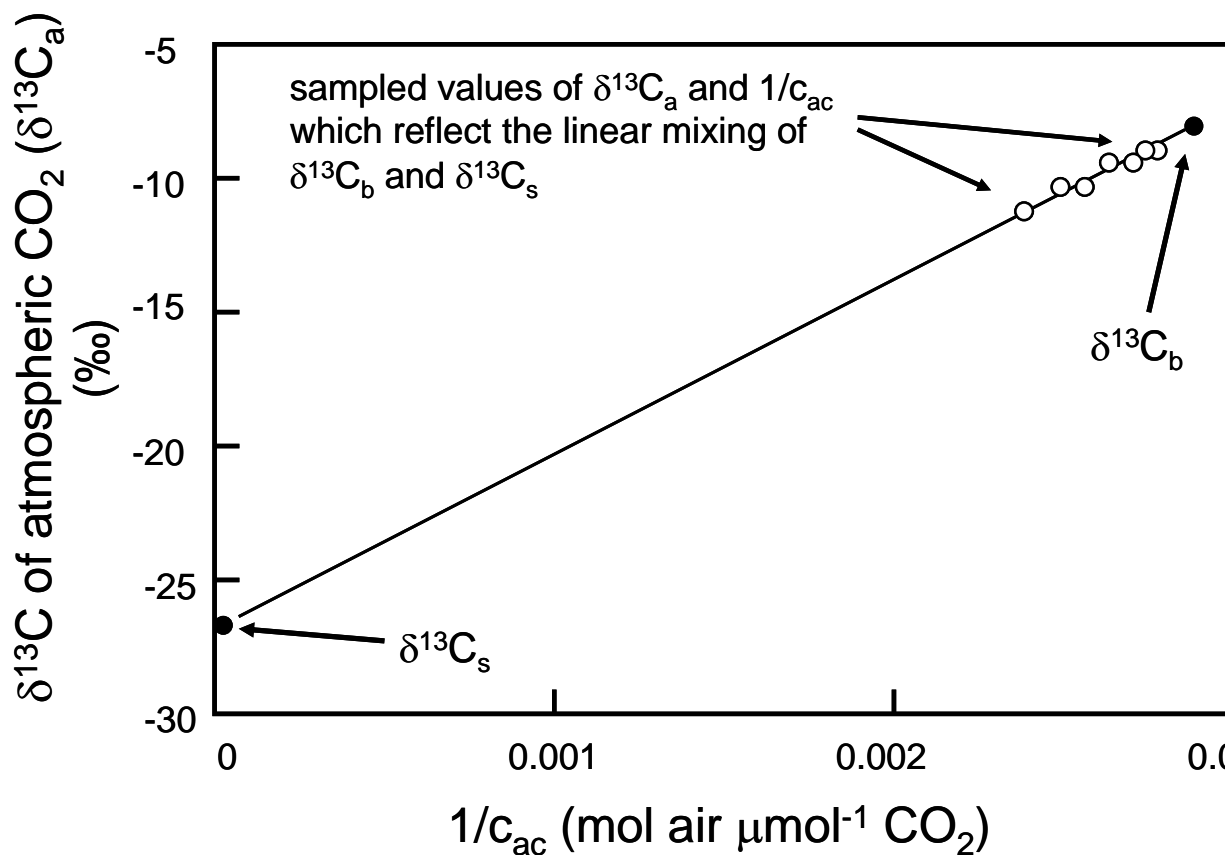


Figure 17.3. A sample nighttime Keeling plot showing the linear regression used to define the two end-member mixing pattern of $\delta^{13}\text{C}_s$ and $\delta^{13}\text{C}_b$ as a function of $1/c_{ac}$. The y-intercept ($\delta^{13}\text{C}_s$) represents the $^{13}\text{C}/^{12}\text{C}$ ratio of the CO_2 source at the lower boundary, and is typically accepted as the $\delta^{13}\text{C}$ of total ecosystem-respired CO_2 . This intercept is often designated as $\delta^{13}\text{C}_R$, rather than $\delta^{13}\text{C}_s$.

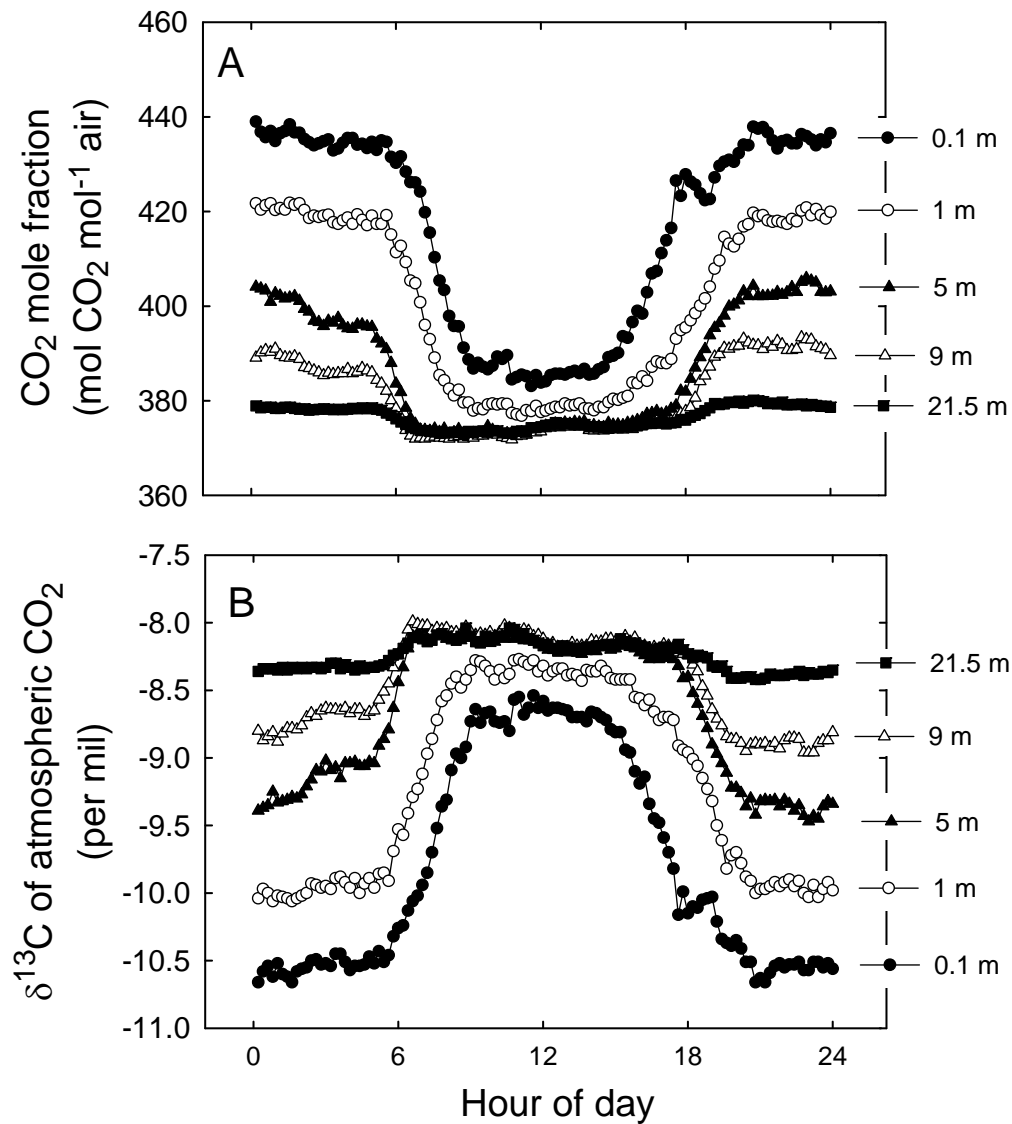


Figure 17.4. **A.** Diurnal variation in the CO₂ mole fraction in air at various heights above a subalpine forest ecosystem in Colorado. **B.** Diurnal variation in the isotopic ratio (¹³C/¹²C) expressed in delta notation, for various heights above a subalpine forest in Colorado. Redrawn from Bowling et al. (2005).

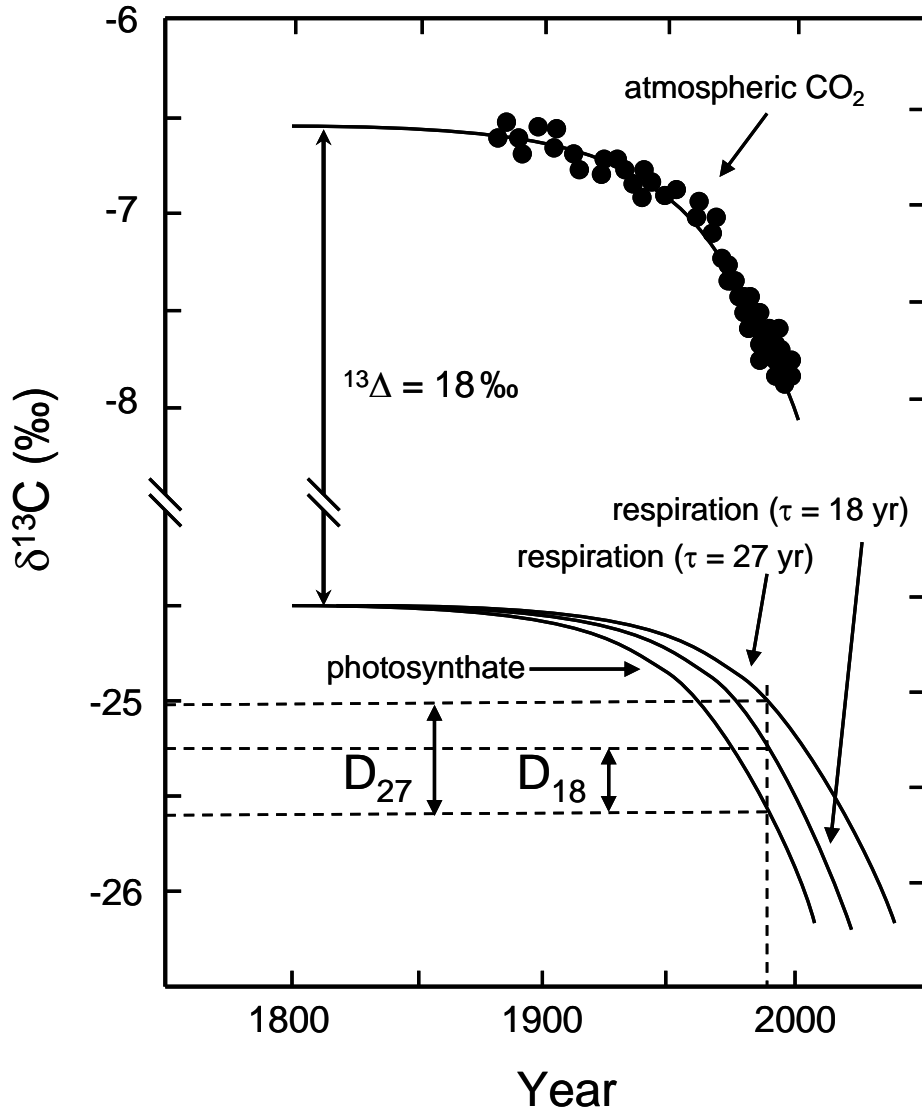


Figure 17.5. Graphic representation of the isotopic disequilibrium between the CO₂ assimilated by photosynthesis and emitted by respiration. The upper line and symbols (for the historical trend in the δ¹³C of atmospheric CO₂) is taken from Francey et al. (1999). We assume a photosynthetic discrimination of 18 ‰, from which we obtain an offset curve labeled here as 'photosynthate'. When the photosynthate curve is offset by 18 years or 27 years, representing estimates of the global mean residence time of assimilated CO₂, we obtain the curves labeled 'τ = 18 yr' and 'τ = 27 yr'. The global mean isotopic disequilibrium that occurs because respiration is offset by 18 or 27 years from photosynthesis is shown as D₁₈ and D₂₇, respectively. Redrawn from a concept presented by Yakir (2004).

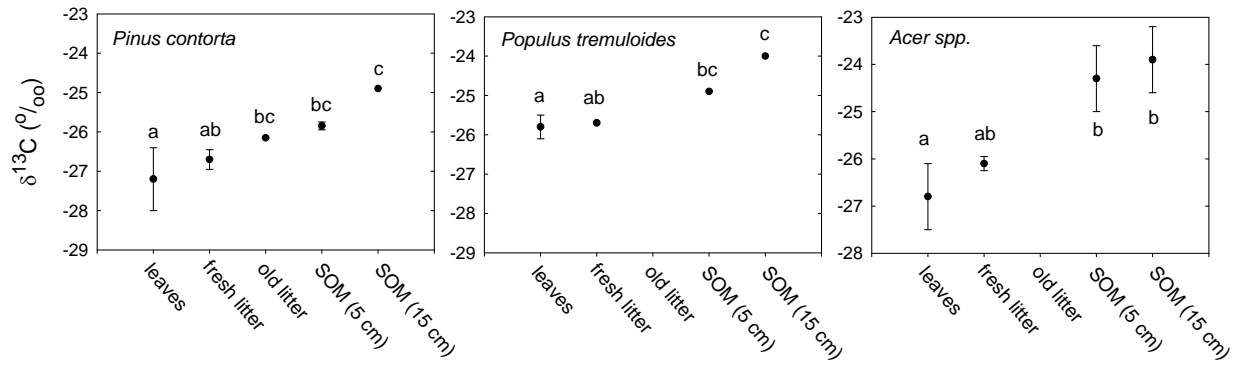


Figure 17.6. Enrichment in ^{13}C in soil litter and SOM at deeper layers of the soil profile in three ecosystems in northern Utah, USA. Vertical bars are ± 1 S.E. and points marked by different letters are statistically significant. Redrawn from Buchmann et al. (1997).

Footnotes (Chapter 17)

¹ The water-splitting reaction of photosynthesis does not discriminate against different isotopic forms of H₂O; so, the isotopic composition of atmospheric O₂ produced from photosynthesis (which is most of the atmospheric O₂) reflects that of the water used. However, the isotopic composition of atmospheric CO₂, and conversely the isotopic composition of biomass, is influenced by photosynthetic discrimination.

² The lowest $\delta^{13}\text{C}_L$ values reported for C₃ leaves – i.e., those that are more negative than -27 ‰ – are typically from shade-grown leaves near the ground, where $\delta^{13}\text{C}_a$ is more negative than -8 ‰ due to the release of ¹³C-depleted CO₂ from the respiration of soil organic matter.

³ Approximately 0.204% of the oxygen isotopes on earth are ¹⁸O, and approximately 0.015% of the hydrogen isotopes are ²H.

⁴ In some derivations, R_E is expressed in terms of the water delivered to the leaf through xylem conduits (e.g., R_X), wherein R_E = R_X. This is a valid equality as long as transpiration is in the steady-state.

⁵ It's important to note that the form of the diffusion equation for gross fluxes differs from that for net fluxes [e.g., A = g_{Lc} (c_{ac} - c_{cc})], in that the gross flux is driven not by the difference in concentration of molecular collisions between two points, but rather by the absolute concentration of molecular collisions at one point.

⁶ The ¹³C/¹²C ratio of the respiration source integrated with respect to all respiration processes with the ecosystem, is often referred to as the $\delta^{13}\text{C}$ of 'ecosystem respiration' and abbreviated as $\delta^{13}\text{C}_R$. We will use $\delta^{13}\text{C}_s$, to indicate the respiratory CO₂ source in our theoretical treatments, but will also refer to this value as $\delta^{13}\text{C}_R$ when discussing general ecosystem carbon cycling.

⁶ The enrichment of atmospheric CO₂ above a canopy in ¹³C during the day is often obscured by atmospheric mixing; but is clearly observed during daylight hours when turbulent mixing is low,

such as in the morning. The depletion of atmospheric above a canopy during the night occurs because SOM, which reflects the product of past photosynthesis with its associated isotope effect, has a lower $^{13}\text{C}/^{12}\text{C}$ ratio than the atmosphere.